Anbar Journal of Engineering Science (AJES) **Vol. 13 , No. 2 (2022) , pp. 122 ~132**
P-ISSN: 1997-9428 ; E-ISSN: 2705-7440 DOI: 10.37649/aengs.2022.176366

Unviersty of Anbar

Anbar Journal of Engineering Science©

journal homepage: https://ajes.uoanbar.edu.iq/

The effect of Corroded Longitudinal Steel Bars on Flexural Behavior of Reinforced Concrete Beams

Tasneem S. Fayaad [a], Yousif A. Mansoor [b], Mahmoud Khashaa Mohammed[C]

[a,b,c]Department of Civil Engineering College of Engineering, University of Anbar, Ramadi, , Iraq

PAPER INFO

Paper history:
Received 21/08/2022
Revised 13/10/2022
Accepted 26/10/2022

Keywords:
tensile steel bar, corrosion, electrochemical accelerated corrosion ,flexural behavior

ABSTRACT

This study aims to examine the relationship between the corrosion rate of longitudinal tensile steel bars and the maximum flexural strength of reinforced concrete RC beams. The study's methodology is designed to show the structural behavior of corroded and non-corroded RC beams, such as ultimate load, deflection, stiffness, crack patterns, and failure mode. Three rectangular beams were cast with dimensions (150× 200 ×1200) mm, and all specimens have the same amount of longitudinal and transverse reinforcement and the same concrete strength. The major parameter is the theoretical mass loss level due to corrosion (0, 10, 15) %. Electrochemical technique was used to accelerate the corrosion in the longitudinal tensile bars. All RC beams were tested under four-point monotonic loading. The test results confirm that the cracking load in corroded beams decreased by 25% comparative to the non- corroded beam. The increase of the percent of corrosion experimental mass loss by 8.25 and 14.15 % decreased the ultimate load by about 14 % and 27%, respectively. This reduction coincided with the decrease in deflection values in mid-span for the ultimate load, which decreased by 53.9% and 46.3%. However, the flexural stiffness was reduced by 13.4 and 15.6% for corroded beams with mass loss (8.25 and 14.15), respectively, compared to the control beam (non-corroded RC beam).

1. Introduction

The corrosion of steel reinforcement is the most deterioration mechanism of reinforced concrete structural members. It is an electrochemical phenomenon in which steel tends to return to its native state (ore) by generating oxides of iron on its surface (rust) [1]. The high pH (12.5) of the concrete hydration products protects the reinforcement steel bars from corrosion. The movement of chlorides' ions through the concrete or carbonation process can reduce the pH of concrete, resulting in an oxidation reaction that produces rust (corrosion can occur at pH values less than 9). The presence of iron oxide layer surrounding the steel at high alkaline nature allows reinforcements to be in passive state [2], [3]. Water and Oxygen are the two main causes of steel corrosion in concrete. However, carbonation and chloride contamination or penetration into the concrete are the main influencing factors that facilitate steel corrosion [4]. Particularly when concrete is exposed to a harsh environment, the corrosion of steel bars is the primary element that affects the serviceability and strength of concrete. The corrosion products (rust) of the steel

* Corresponding author: Tasneem S. Fayaad; tas20e1003@uoanbar.edu.iq ; +9647810695956

reinforcement expand to many times their original size, creating high pressures within the concrete that lead to cracking and spalling of the concrete cover. Expose the rebar to further corrosion activity reduces the structure's capacity to carry load and serviceability [5]. Approximately 80% of the damage observed in existing concrete structures is attributable to steel reinforcement corrosion. Typical corrosion-related phenomena that influence structural capacity include: (i) steel cross-section and ductility reduction, (ii) concrete cracking, (iii) concrete area reduction resulting from spalling, and (iv) change of concrete-steel bond strength properties [6]. Other parameters can affect the steel corrosion in concrete, such as water/cement, type of binder, degree of compaction, compressive strength, and curing of concrete. In concrete, the capillary pores determine the transport properties, such as gas and ion diffusion, water and other fluid capillary suction, and gas and fluid permeability [7]. In past, there have been many studies about the structural behavior of R.C corroded beams. Cairns and Zhao, in 1993 [24], found that the ultimate flexural strength decreased by twenty percent when sixty percent of the length of tensile bars had been exposed to corrosion. When the unbound length exceeded 90 percent of the tensile bar's length, the flexural strength was reduced by 50 % [8]. Fang et al., in 2004 [9], concluded that at 9% mass loss, the decrease in bond strength for deformed steel bars was around 65%. Peng et al., in 2017[10] described the experimental findings regarding the mechanical behavior of corroded reinforced concrete beams. Three beams had been corroded to a degree of 10% mass loss by means of an impressed electrical current. Different cover thickness was used 25, 30 and 35 mm. The details of the specimens are: each specimen was (1,800× 150 ×300) mm with a rectangular cross-section and reinforced by two 22mm diameter bottom longitudinal deformed reinforcing bars, two 16mm diameter top longitudinal deformed reinforcing bars. The study found that the ultimate strength decreases when the rates of corrosion increase while the ultimate deflection for corrosion beams increase when the degree of corrosion increase. However, the actual corrosion rates were 12.9%, 8%, and 8% for beams C10C25, C10C30 and C10C35, respectively. The test results confirm that the beam with 8% corrosion has a 5.6% lower ultimate load at failure than that for the control beam without corrosion. However, the specimen C10C25 has very brittle behavior compared with beams C10C30 and C10C35. This is because the first has higher corrosion rate. Other research by Patil et al. in 2018[5] used a pull-out test to study the impact of reinforcing bar corrosion and cracking on reinforced concrete member bond strength. Bond behavior is investigated at various levels of reinforcement bar corrosion in 30 specimens. These corrosion stages were achieved by impressing direct current for a longer period of time on the reinforcing bar embedded in the pull-out specimen immersed in 5% NaCl solution. Each concrete cylinder in this study has one deformed bar of ϕ12 mm in its center. The author observed that at 10% corrosion rate, the bond strength was reduced by 31%. However, a decrease in bond strength not only affected the ultimate loads and service lives of the elements, but also it changed the mode of failure by converting it from ductile to tragic brittle one. A more recent study by Yuan et al. in 2021 [11] investigated the mechanical properties of corroded RC beams exposed to electrochemical corrosion. They clarified that the corrosion not only decreases mechanical reinforcement properties but also weakens reinforcement adhesion with the concrete, diminishes RC beam stiffness and ultimate load-bearing capacity, and impedes the concrete's compression performance. Corrosion hastens crack development and beam failure. Mahmood and Lateef, in 2021[12], investigated the effect of corroded steel bars on the ultimate flexural capacity of reinforced concrete beams. Four RC beams (150, 200, and 1200 mm) were examined in this experiment under a two-point concentrated load. These were cast using 30 MPa compressive strength concrete. Longitudinal rebar with 2ϕ 8mm was used in the tension and compression zones, and 6mm stirrups with 100 mm c/c spacing were employed (shear reinforcement). The corrosion period (5,10,20) days is the primary parameter of this study. All samples had the same amount of longitudinal and transverse reinforcement, concrete strength, and other variables. The results of the tests indicated that the ultimate loads for corrosion durations of 5, 10, and 20 days drop by 2.44, 11.1, and 16.0%, respectively relative to the control beam owing to corrosion damage. However, in comparison to the control beam, the deflection at mid-span for ultimate loads reduced by approximately (9.32, 24.65, and 36.65 %) for (5, 10, 20) days, respectively. From the foregoing, it can be seen that there was no

agreement between researchers about the exact effect of steel reinforcement corrosion on bending behavior of RC beams. There is no accurate visualization to know the decrease in RC beams' maximum capacity and its ductility due to corrosion. Therefore, this research aims to determine the exact drawback in the bending strength due to corrosion which may help in re-calculating the design loads of degradations beams. This will be very helpful in the selection and design of suitable way for strengthening based on the assessment of the degree of corrosion and the extent of damage resulting from this corrosion.

2. Experimental Program

2.1 Materials properties

Ordinary Portland Cement (Type I) was used. It has a specific gravity of 3.15, a Specific surface area of 314 (kg /m^2), Initial and final setting of 126,228 min, respectively. Cement's chemical and physical properties were tested and identical to Iraqi specification IQS NO. 5, 2019[13].

Fine and coarse aggregate: Locally natural fine aggregate with a maximum size of 4.75 mm and a specific gravity of 2.62 was used. Naturally rounded coarse aggregate with a maximum size of 10 mm and a specific gravity of 2.6 was used. Sieve analysis results were within the limits of the Iraqi specification IQ. S 45/1984[14].

Deformed steel bars with diameters (ϕ12, ϕ8, ϕ6) mm were used to reinforce concrete beams. The mechanical properties of reinforced steel bars are shown in Table 1, which conform to the ASTM A61 requirements [15].

Table 1. Properties of steel reinforcement

Nominal diameter (mm)	Actual diameter (mm)	Actual cross section area (mm^2)	Yield Stress(N/mm)	Elongation (%)
6	5.6	23.758	509	7.5
8	7.7	46.566	519	11
12	11.3	100.287	640	11.8

2.2 Beam specimen details

The beams were designed to make the shear capacity greater than the flexural capacity in the original beams, according to the American Concrete Institute ACI 318M-19code [16]. Two deformed bars with a diameter of 12 mm and a length of 1400 mm were used to reinforce the beams in the tension zone. The top steel reinforcement was two bars of length 1360 mm with diameters of 6 mm and deformed stirrups bars of 8 mm diameter at spacing 80 mm center to center.

The specimen cross-section details are illustrated in Figure 1. All stirrups were protected by epoxy to prevent further corrosion of steel stirrups. The plastic tape was warped at the connection area between the stirrups and longitudinal bars. The concrete cover is 20 mm, and all longitudinal bars subjected to corrosion are warped by stripped wire to represent an anode (source of an electron acceptor).

2.3 Concrete mix design

The concrete mixture was designed according to the American Concrete Institute method [ACI211] [17] to determine the concrete's design properties, such as workability, compressive strength, and other hardened properties. The mixture was of 400 kg/m3 cement content,750 kg/m3 fine aggregate, 1050 kg/m3 coarse aggregate, and 190 kg/m3 water. The workability for the normal concrete was tested by slump test, which was 90 mm.

2.4 Mechanical properties of concrete mix

The specimens were cast concurrently with mixing and casting beams to determine the concrete mix's mechanical properties.

The ELE-Digital testing compression machine with a maximum capacity of 2000 kN was used to assess the average strength of 3 cylinders with

dimensions (150× 300) mm according to ASTM C39-05 [18] at a rate of 5.30 kN/s.

In the same compressive strength machine with a rate of 0.94 kN/s, splitting strength was tested following ASTM C496-11[19] for three cylinders with dimensions (100×200) mm. Three prisms (100 ×100 ×400) mm tested based on the ASTM C78-15 standard [20] to determine the modulus of rupture. The flexural strength or modulus of rupture was measured using a hydraulic fracture machine with a capacity of 200 kN.

Also, a cylinder with dimensions (150 ×300) mm, based on the ASTM C469-02 [21], was used to determine Young's modulus in a compressive test machine with a loading rate of 5.3 kN/s. These properties are presented in Table 2.

Table 2. Mechanical properties of concrete mix

Compressive strength ($f'c$) (MPa)	Splitting tensile strength (MPa)	Flexural strength(MPa)	Modulus of elasticity (MPa)
33	4	6.5	27000

2.5 Corrosion process cell

Electrochemical technique was used to accelerate mass loss in longitudinal bars after the curing process. Three corrosion levels were used for this experiment (0, 10, 15) % mass losses; however, the beam samples were identified as RM0, RM10, and RM15, respectively.

An external source (DC) power supply was used to apply an electrical current to the longitudinal tensile bars. To maintain a moist environment around and inside the specimens, the specimens were immersed in a salt solution of 5% NaCl for 24 hours, about 130 mm from the top of the specimen, before beginning electrochemical corrosion.

The inserted tensile longitudinal bars were connected to the positive terminal of the (DC) power supply via an electrical cable to serve as an anode, as shown in Figure 2. As a cathode, exterior stainless steel plates with a length of 1000 mm and height of 200 mm, linked to the negative terminal of a voltmeter, were put at the sides of each specimen. They were connected in series.

The (DC) current source was used to apply a current density of 2 mA/cm^2 to the embedding steel bars based on the surface area. Each tensile rebar in the beam was approximately required 1.055 A. Faraday's law had been utilized as a theoretical guide to determine the needed time to cause corrosion damage [22], [23], [24] [25], [26].

2.6 Corrosion cracks examination process

Cracks had formed on the concrete's surface due to the corrosion process, and they were primarily aligned with the placement of the tensile longitudinal bars. Rust staining is caused by steel dissolving at the metal/oxide contact.

To measure the width of corrosion cracks, the rust was first cleaned with water and a nonmetals brush, then the corrosion cracks' pattern was deduced. Three surfaces of corroded beams were mapped using a 50 ×50 mm grid. The corrosion crack widths were investigated by the Microscope Micrometer Calibration Ruler, see Figure 3.

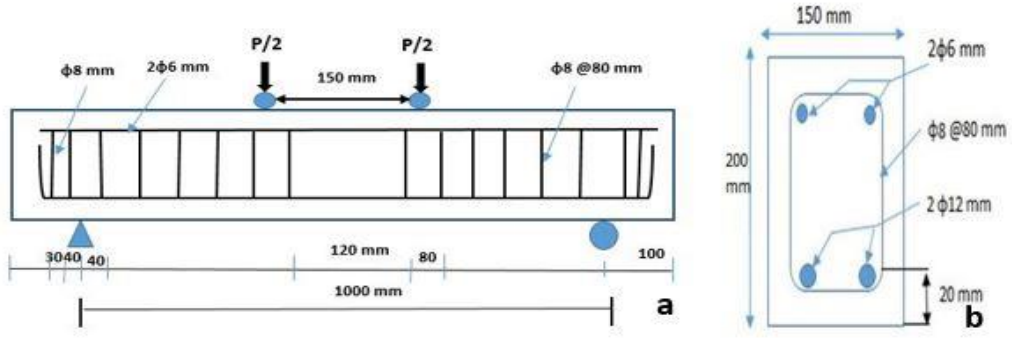

Figure 1. Beam Reinforcement Details **(a)** Longitudinal View **(b)** Cross Section

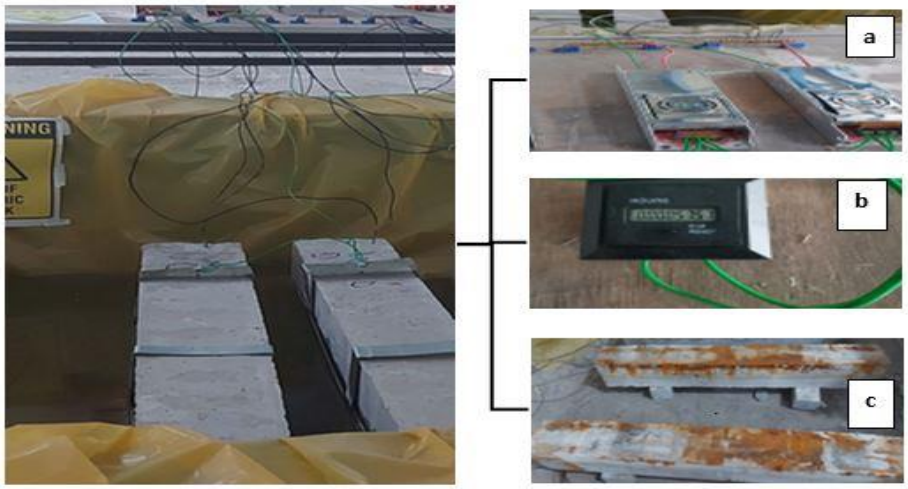

Figure 2. Setup for Accelerated Corrosion**. (a)** The (DC) power supply**(b)**Timer**(c)**Deterioration beams at the end of accelerated corrosion process

Figure 3. The corrosion crack widths investigating procedures

2.7 Testing of beam specimens

A machine with a maximum capacity of 400 kN was used for testing concrete beams, as shown in Figure 4. It was used to test simply supported beams with a total and clear span length of 1000 mm. The test of beams was performed with a loading rate of 0.5 kN/sec, and the two loading point's plate was placed in the middle of the clear span with a distance of 150 mm between them. Five LVDTs (deflection gauges) were used below every beam with an accuracy of 1×10^{-18} mm, three with a capacity of 100 mm put in the middle of the beam, two under load points, and one between them at mid-span. The rest two have a capacity of 50 mm and were located nearby supports at a distance of 200 mm each.

Figure 4. Testing Machine

2.8 Evaluation the Mass Loss

After structural testing completed, the mass losses for corroded longitudinal rebars were evaluated using distractive technique. The corroded beams were broken using hand held electric percussion to exert the corroded rebars and cleaning according to the stranded procedure of ASTM G1-3 [23].

The rust product was removed firstly from them by metal brash to remove the weak surface and attached concrete mortar. Then, chemical cleaning was done by placing them in a chemical solution contains high concentration of HCl acid. Finally, the samples were weighed to determine the amount of steel loss (mass loss) in digital balance. Each bar mass loss % was calculated according to the following equation:

$$\text{Mass loss \%} = \frac{Mass\ Before\ Corrosion(Kg) - Mass\ After\ Corrosion(Kg)}{Mass\ Before\ Corrosion(Kg)} * 100 \quad ..(1)$$

3. Results and Discussion

3.1 Mass Loss and Cracking Patterns Due to Corrosion

The mass loss percent and maximum corrosion-cracks width present Table 3. As the longitudinal bars subjected to corrosion, corrosion products achieve at the steel's surface that occupied a large volume, resulting in internal hooping stress, causing a crack. Therefore, the horizontal cracks were mainly formed in parallel with a longitudinal bars' planes. This occurred because the radial stress induced by the corrosion. For more description, the typical cracks patterns for the corroded beams at three sides (front, rear, and bottom) were presented as schematic drawings. Figure 5 and Figure 6 show the crack patterns for beams RM10 and RM15 respectively.

3.2 Flexural test results

The experimental setup test results summarized in Table 4 which includes: load at first flexural crack (Pcr), ultimate load (Pu), deflection at first crack (Δcr), deflection at ultimate load (Δu), the mass losses of tensile longitudinal bars of corroded beams.

In addition, the maximum crack width measured for the larger crack on the beam's face at failure are also reported. This width, in fact, represents the full load since the cracks have reached this width by continuing loading until the ultimate value. The first cracking load was recorded as the load applied on the specimen corresponding to the first visible crack by human eye.

Table 3. Mass loss and maximum corrosion crack width

Specimen	Mass loss %

	Bar No.	Theoretical %	Experimental %	Average %	Maximum Crack width (mm)
RM10	B1	10	8.1	8.25	0.4
	B2		8.4		
RM15	B1	15	14.06	14.15	0.45
	B2		14.24		

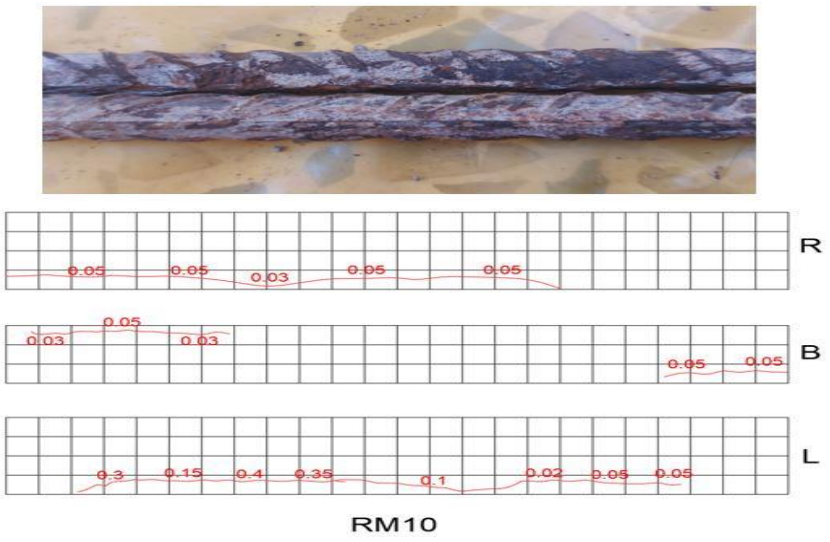

Figure 5. Patterns of corrosion induce crack of Beam RM10 (unit: mm)

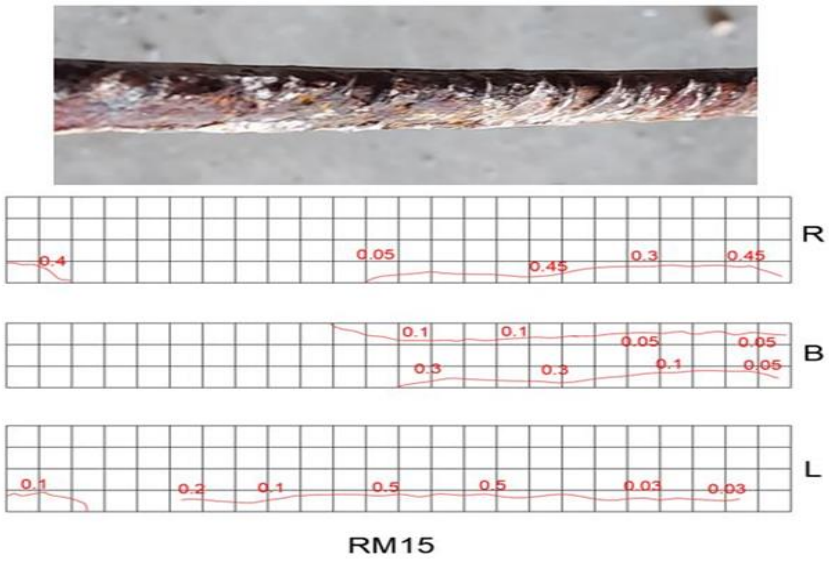

Figure 6. Patterns of Corrosion Induce Crack of Beam RM15 (unit: mm)

Table 4. The experimental test results

Beam ID	Corrosion mass loss (%)	Ultimate Load(Pu) (KN)	Load at First crack (pcr)(KN)	Pcr/Pu (%)	Change percent in Pu with respect to	Def. @ ultimate load (Δu)	Def. @ cracked load (Δcr)	Maximum crack width at failure (mm)
RM0	-	120	40	33	Ref.	8.831	0.93	1.95
RM10	8.25	103.17	30	29	-14	4.068	0.73	1.4
RM15	14.15	87.47	30	34	-27	4.743	0.83	1

3.2.1 Load-deflection Relationship

Figure 7 shows the response of the load-mid span deflection plot of the beams. The results showed that the peak load degraded significantly by about (14 and 27%) with the increase of corrosion mass loss percent in beams RM10 and RM15 by 8.25 and 14.15 %, respectively, compared to beam RM0, which has an ultimate load of 120 kN. These results are in agreement with other researchers, Acosta et al. [27], Triantafyllou et al. [28], Hu et al. [11], and Mahmood and Lateef [14].

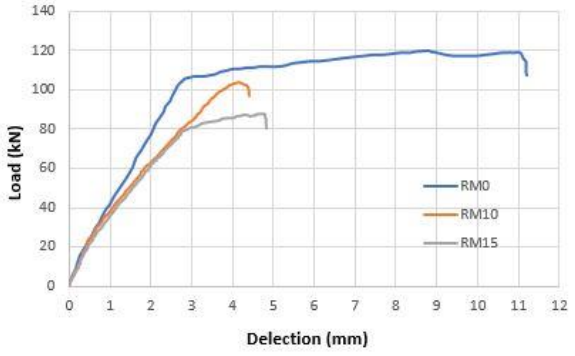

Figure 7. Effect of Corrosion mass loss percent on the load-deflection behavior

In contrast, the deflection value in the mid-span for ultimate loads decreased by (53.9 and 46.3) % for corroded damage beams (RM10) and (RM15), respectively, relative to the control beam (RM0). This was compatible with that obtained by Abdel Mohti and Shen [29], Hu et al. [11], Mahmood and Lateef [14], and Zhang et al. [12], [25], [30]. The prominent behavior afterward of the deflection of the beam (RM15) tends to increase slightly than the beam (RM10) until failure. It is speculated that when the corrosion rate exceeds 10%, the bond strength between the reinforcing bar and the concrete is insufficient, leading to an increase in the ultimate deflection. This behavior was noticed by Zhang et al., 2021 [30].

In addition, the effect of the corrosion on the cracking load was observed, as it decreased by 25% compared to the control beam RM0. The experimental results demonstrated that the corroded RC beam exhibited a less ductile failure mode than a control beam of the same age. This might be due to the difference in mechanical properties between corroded and non-corroded steel bars.

3.2.2 Flexural Stiffness

The flexural stiffness (k) was determined by calculating the slope (ΔF/Δδ) of the linear portion of the load-deflection curves between (10% and 50%) of the maximum load, Najim, 2012 [31]. Table 5 shows the stiffness of tested beams, and Figure 8 shows a comparison in stiffness values of tested beams.

The stiffness of beams RM10 and RM15 decreased by 13.4 and 15.6% with mass loss percent of 8.25 and 14.15 %, respectively, related to non-corroded reference beam RM0. It is evident from Figure 8 that the flexural stiffness of beam RM10 and beam RM15 was very close, despite the difference between corrosion ratios and bearing capacity. This confirms the previous study [32].

It has been concluded that the flexural stiffness derived from beam defects decreased sharply during the early corrosion stages (5–8% steel mass

loss) and remained constant despite the steel corrosion level continuing to increase. Consequently, stiffness can be used as an indication of the level of steel corrosion during its early stages. However, the level of steel corrosion at which stiffness remained constant despite an ongoing increase in the level of corrosion is insufficiently high.

Table 5. Stiffness of tested beams

Beam ID	Stiffness (kN/mm)
RM0	35.8
RM10	31
RM15	30.2

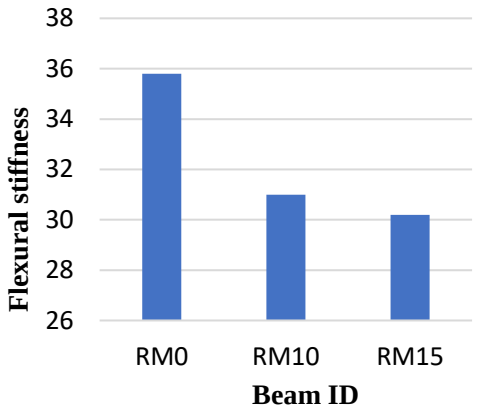

Figure 8. Effect of mass loss percent on Beams flexural stiffness

3.2.3 Crack patterns and failure modes

The failure load was defined in this investigation as the load equivalent to the greatest applied static load beyond which the beam experienced a substantial loss in strength and ultimately collapsed.

In all tested beams failure was by cracks that started from the beam soffit at the largest bending moment, these cracks progressed toward the top zone as a result of steel yielding (flexural failure). The flexural failure is most common failure for Reinforced concrete beams because the designer avoided the shear failure.

Therefore, the study shows the corrosion damages on flexural behavior of R.C beams. It is clear that the first visible crack appeared near the bending zone in the middle of the beam. First, perpendicular cracks appeared on the tension of the area under the neutral axis of the sample as a result of tensile stresses exceeding the concrete's tensile strength.

As these cracks spread, they became more complicated as the loading process moved forward. Due to the high-stress level in the tension area, these cracks flitted up to the compression zone by continuing the loading process to the top edge near the applied load area. Figures 9 to 11 show the cracks at the failure of the tested beams.

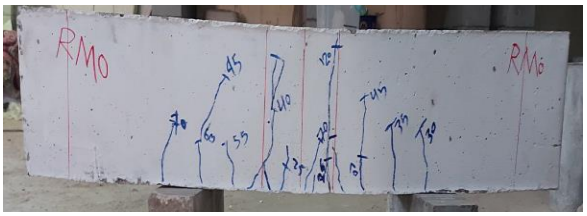

Figure 9. Cracks at the failure of the RM0 beam.

Figure 10. Cracks at the failure of the RM10 beam.

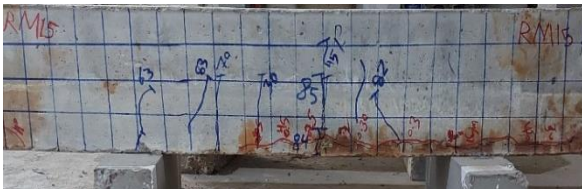

Figure 11. Cracks at the failure of the RM15 beam

8. Conclusion

The Behavior of reinforced concrete beams subjected to accelerated corrosion in longitudinal bars was investigated in this paper. The main conclusions could be summarized as follows:

- Accelerated corrosion process caused a decrease in the weight of steel bars by (8.25,14.15) % which presented 10% and 15% theoretical mass loss.
- The load-deflection relationship, showed that the percent of corrosion mass loss significantly impacts on the ultimate load; the increase of the percent of corrosion mass loss by 8.25 and 14.15 % decreased the failure load by about (14 % and 27%), respectively. This exact determination of reductions helped in selection and design of proper strengthening technique for next stage of this research in future.
- The deflection value in mid-span for ultimate loads reduction by (53.9 and 46.3) % of corroded damage beams with actual mass loss ratio by 8.25% and 14.15 %, respectively.
- After the occurrence of corrosion, the cracking load in corroded beams with actual mass loss ratio by 8.25% and 14.15 %, decreased by 25% comparative to the non- corroded beam.
- The stiffness decreased by 13.4 and 15.6%, related to non- corroded reference beam, with the increase of the percent of corrosion mass loss by 8.25 and 14.15 %, respectively.
- For all tested beams, the failure mode was a flexural failure, and the cracking pattern spread between the two-point load's zone and shear span.

References

[1] K. Koulouris and C. Apostolopoulos, "An experimental study on effects of corrosion and stirrups spacing on bond behavior of reinforced concrete," Metals (Basel)., vol. 10, no. 10, pp. 1–14, 2020, doi: 10.3390/met10101327.

[2] P. Ghoddousi, M. Haghtalab, and A. A. Shirzadi Javid, "Experimental and numerical analysis of the effects of different repair mortars on the controlling factors of macro-cell corrosion in concrete patch repair," Cem. Concr. Compos., vol. 121, p. 104077, Aug. 2021, doi: 10.1016/J.CEMCONCOMP.2021.104077.

[3] A. reza Kashani and T. Ngo, Self-Compacting Concrete: Materials, Properties, and Applications. A volume in Wood-head Publishing Series in Civil and Structural Engineering, Book, 2020.

[4] U. Angst, Ueli Angst Chloride induced reinforcement corrosion in concrete, no. January. 2011.

[5] A. N. Patil, B. G. Birajdar, and H. K. Erande, "Study of Influence of Corrosion and Cracking on Bond Behavior of Reinforced Concrete Member," no. September 2017, 2018.

[6] A. Kagermanov and I. Markovic, "FE-Modelling Techniques for Structural Capacity Assessment of Corroded FE-Modelling Techniques for Structural Capacity Assessment of Corroded Reinforced Concrete Structures .," no. September, pp. 1–8, 2019.

[7] H. – W. Reinhardt, "Corrosion protection of reinforcing steels," 2009.

[8] J. Cairns and Z. Zhao, "Behaviour of concrete beams with exposed reinforcement., "Proc. Inst. Civ. Eng. Build., vol. 99, no. 2, pp. 141–154, 1993.

[9] C. Fang, K. Lundgren, L. Chen, and C. Zhu, "Corrosion influence on bond in reinforced concrete, " Cem. Concr. Res., vol. 34, no. 11, pp. 2159–2167, 2004.

[10] J. Peng, H. Tang, and J. Zhang, "Structural Behavior of Corroded Reinforced Concrete Beams Strengthened with Steel Plate," J. Perform. Constr. Facil., vol. 31, no. 4, 2017, doi: 10.1061/(asce)cf.1943-5509.0001004.

[11] P. Yuan, L. Xiao, X. Wang, and G. Xu, "Failure mechanism of corroded RC beams strengthened at shear and bending positions," Eng. Struct., vol. 240, no. April, p. 112382, 2021, doi: 10.1016/j.engstruct.2021.112382.

[12] N. Mahmood and A. Lateef, "Effect of Corrosion Longitudinal Steel Bars on the Flexural Strength of Rc Beams," Tikrit J. Eng. Sci., vol. 28, no. 2, pp. 44–53, 2021, doi: 10.25130/tjes.28.2.04.

[13] Iraqi Specifications No. (5), 2019 for Portland Cement requirements. .

[14] IQS NO. 45, 1984, "Aggregate from Natural Sources for Concrete and Construction. Central Agency for Standardization and Quality Control", Baghdad, Iraq. .

[15] ASTM, "Standard Specification for Deformed and Plain Carbon Steel Bars for Concrete," B. Stand. Vol. 01.04, pp. 1–6, 2004.

[16] ACI 318-19, Building Code (ACI 318-19)

and Commentary on Building Code Requirements for Structural Concrete (ACI 318R-19). 2019.

[17] A. C. A. C. 211 211, Standard Practice for Selecting Proportions for Normal, Heavyweight, and Mass Concrete (ACI 211.1-91) Donald, no. 9. 2006, pp. 120–121.

[18] ASTM C39/C39M-05. Standard Test Method for Compressive Strength of Cylindrical Concrete Specimens. ASTM Int. 2005; 1– 8. .

[19] ASTM C496/C496M-11. Standard Test Method for Splitting Tensile Strength of Cylindrical Concrete Specimens. ASTM Stand. Vol. 04.02. 2011;1–5. .

[20] ASTM C78-15. Standard test method for flexural strength of concrete (using simple beam with third-point loading). American Society for Testing and Material. 2015. .

[21] ASTM C469-02. Standard Test Method for Static Modulus of Elasticity and Poisson's Ratio of Concrete in Compression. ASTM Stand. B., vol. 04.2002;1–5. .

[22] M. Sahmaran, O. Anil, M. Lachemi, G. Yildirim, A. F. Ashour, and F. Acar, "Effect of corrosion on shear behavior of reinforced engineered cementitious composite beams, " ACI Struct. J., vol. 112, no. 6, pp. 771–782, 2015.

[23] B. Almassri, A. Kreit, F. Al Mahmoud, and R. Francois, "Behaviour of corroded shearcritical reinforced concrete beams repaired with NSM CFRP rods, " Compos. Struct., vol. 123, pp. 204–215, 2015.

[24] Z. Ye, W. Zhang, and X. Gu, " Deterioration of shear behavior of corroded reinforced concrete beams, " Eng. Struct., vol. 168, no. May, pp. 708–720, 2018.

[25] B. Hu, Y. Zhou, F. Xing, L. Sui, and M. Luo, "Experimental and theoretical investigation on the hybrid CFRP-ECC flexural strengthening of RC beams with corroded longitudinal reinforcement," Eng. Struct., vol. 200, no. April, p. 109717, 2019, doi: 10.1016/j.engstruct.2019.109717.

[26] H. Shabani Attar, M. Reza Esfahani, and A. Ramezani, "Experimental investigation of flexural and shear strengthening of RC beams using fiber-reinforced self-consolidating concrete jackets," Structures, vol. 27, no. May, pp. 46–53, 2020, doi: 10.1016/j.istruc.2020.05.032.

[27] A. A. Torres-Acosta, S. Navarro-Gutierrez, and J. Terán-Guillén, "Residual flexure capacity of corroded reinforced concrete beams," Eng. Struct., vol. 29, no. 6, pp. 1145–1152, 2007, doi: 10.1016/j.engstruct.2006.07.018.

[28] G.G. Triantafyllou, T.C. Rousakis, A.I. Karabinis, "Effect of patch repair and strengthening with EBR and NSM CFRP laminates for RC beams with low, medium and heavy corrosion, " Compos. B Eng. 133 (2018) 101–111.

[29] A. Abdel-Mohti and H. Shen, "Strengthening of corroded reinforced SCC-RAP members with CFRP," *Fibers*, vol. 4, no. 1, pp. 1–24, 2016, doi: 10.3390/fib4010003.

[30] T. Zhang, L. Xu, P. Li, and H. Chen, "Numerical Simulation Analysis for Mechanical Properties of Corroded Reinforced Concrete Beams," vol. 4, no. 7, pp. 44–50, 2021, doi: 10.25236/AJETS.2021.040708.

[31] K. Najim, "Mechanics and Structures Determination and Enhancement of Mechanical and Thermo-physical Behaviour of Crumb Rubber-modified Structural Concrete Khalid Battal Najim , BSc Eng ., MSc Eng .," no. January 2012, 2013.

[32] G. Malumbela, P. Moyo, and M. Alexander, "Longitudinal strains and stiffness of RC beams under load as measures of corrosion levels," *Eng. Struct.*, vol. 35, pp. 215–227, 2012, doi: 10.1016/j.engstruct.2011.11.021.